

LONGITUDINAL PHASE SPACE TOMOGRAPHY USING A BOOSTER CAVITY AT THE PHOTO INJECTOR TEST FACILITY AT DESY, ZEUTHEN SITE (PITZ)

D. Malyutin*, M. Gross, I. Isaev, M. Khojayan, G. Kourkafas, M. Krasilnikov, B. Marchetti, F. Stephan, G. Vashchenko, DESY, 15738 Zeuthen, Germany

Abstract

One of the ways to measure the longitudinal phase space of the electron bunch in a linear accelerator is a tomographic technique based on measurements of the bunch momentum spectra while varying the bunch energy chirp. The energy chirp at PITZ can be controlled by varying the RF phase of the CDS booster – the accelerating structure installed downstream the electron source (RF gun). The resulting momentum distribution can be measured with a dipole spectrometer downstream. As a result, the longitudinal phase space at the entrance of the CDS booster can be reconstructed.

In this paper the tomographic technique for longitudinal phase space measurements is described. Results of measurements at PITZ are presented and discussed.

tomographic technique [3, 4]. Both methods allow full longitudinal phase space characterization. With the current setup of the Photo Injector Test facility at DESY, Zeuthen site (PITZ), only the tomographic technique can be employed. A TDS, which is already installed in the beamline, is planned to be put into operation at the end of this year.

The PITZ facility was built as an electron source test stand [5] for FELs like FLASH and the European XFEL. The present PITZ beamline layout is shown in Fig. 1. The main components of the PITZ facility are a photocathode laser system, an RF photo-electron gun (first accelerating structure) surrounded by main and a bucking solenoids, a second accelerating structure – Cut Disk Structure (CDS) which is also called booster cavity; and three dipole spectrometers. One spectrometer is located in the low energy section downstream the gun (Low Energy Dispersive Arm – LEDA), a second one in the high energy section downstream the booster (the first High Energy Dispersive Arm – HEDA1), and the third one in the end of the PITZ beamline (the second High Energy Dispersive Arm – HEDA2). Additionally there are three Emittance Measurement Stations (EMSYs) and a transverse deflecting structure (TDS), Fig. 1.

INTRODUCTION

For successful operation of linac based Free Electron Lasers (FELs) there are quite stringent requirements on the electron beam quality: small transverse emittance, small energy spread and high beam peak current (high brightness) [1]. The measurements of the beam slice energy spread and current profile can be done using a transverse deflecting structure (TDS) [2] or using a

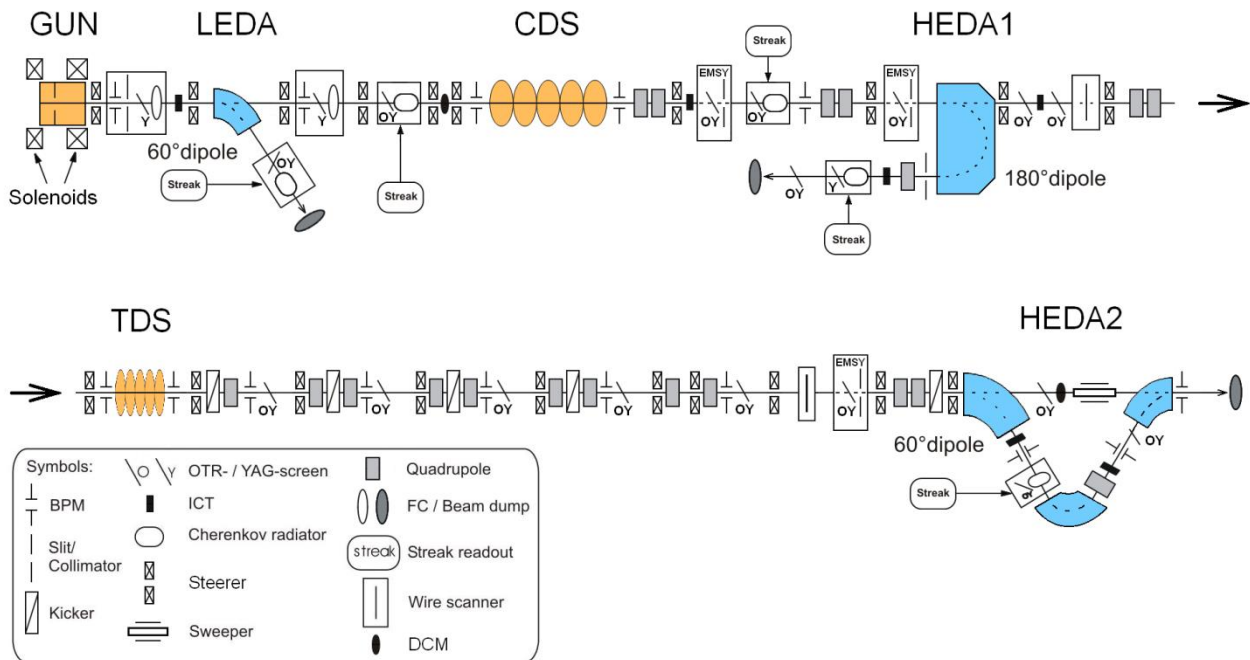


Figure 1: PITZ beamline layout. The beam propagates from left to right.

*dmitriy.malyutin@desy.de

LONGITUDINAL PHASE SPACE TOMOGRAPHY

A tomographic technique can be used for measuring of the longitudinal phase space as the input projections for the reconstruction will correspond to momentum spectra where the bunch energy chirp has been varied [3]. The electron bunch current profile and slice energy spread can be extracted from the reconstructed longitudinal phase space and the longitudinal emittance can be calculated as well.

At PITZ, such measurements can be performed by varying the RF phase of the CDS booster. The momentum spectra measured downstream the booster at the HEDA1 or HEDA2 dispersive sections can be used to feed the tomographic reconstruction. Finally, the longitudinal phase space can be reconstructed using for example the Algebraic Reconstruction Technique (ART) [6].

Bunch Momentum Chirp

The acceleration of an ultra-relativistic electron bunch in an accelerating structure can be described as [7]:

$$p = p_0 + V \cdot \cos(\varphi), \quad (1)$$

where p_0 is the bunch initial momentum, V is the maximum momentum gain by the accelerating structure, φ is the RF phase of the structure relative to the maximum mean momentum gain (MMM) phase and p is the bunch final momentum.

The bunch momentum chirp k induced by an accelerating structure can be calculated from Eq. (1) as a first time derivative with inverse sign:

$$k = -\frac{dp}{dt} = V\omega \cdot \sin(\varphi), \quad (2)$$

where $\omega = 2\pi f$ and f is the RF frequency in the structure.

Since the acceleration by the accelerating structure cannot cause full 90° rotation of the longitudinal phase space, the temporal resolution will be limited by the maximum momentum chirp applied to the bunch, the slice momentum spread in the bunch and the momentum resolution of the momentum distribution measurement system. The time resolution σ_t can be roughly estimated from the maximum momentum chirp k_{\max} applied to the bunch:

$$\sigma_t = \frac{\sigma_\delta}{k_{\max}}, \quad (3)$$

where σ_δ is the electron bunch slice momentum spread. Here it is assumed that the resolution of the momentum measurement is much better (smaller) than the bunch slice momentum spread.

Bunch Length Estimation

The electron bunch length can quickly be estimated from the momentum phase scan without performing the time consuming tomographic reconstruction. But such estimation will be rough. For this one need to make maximum momentum spread of the bunch by going to the off-crest RF phase of the accelerating structure, which is

still measurable by a dispersive section (spectrometer). Measuring this momentum spread the bunch length can be calculated by:

$$\delta_l = \frac{\delta_p}{k_0 + k_1} c, \quad (4)$$

where δ_l is the RMS bunch length, δ_p is the RMS momentum spread, k_0 is the initial momentum chirp (upstream the booster), k_1 is the momentum chirp induced by the booster cavity at the maximum measurable momentum spread and c is the speed of light. k_0 can be estimated using Eq. (2) with inverse sign at the phase with minimum momentum spread.

EXPERIMENTAL RESULTS

Experimental measurements of the longitudinal phase space were performed at PITZ for two laser temporal profiles Gaussian and flat-top. For each case the range of booster RF phases was chosen to have measurable bunch momentum distributions in the dispersive section (enough high intensity and bunch size within the observation screen) and usually it is chosen at about ± 20 degrees around the MMMG phase.

For the first set of measurements a bunch charge of 20 pC was chosen and the photo cathode laser had a Gaussian temporal profile with FWHM length of 2.8 ps. Figure 2 shows the measured mean beam momentum and RMS momentum spread in the HEDA1 section as a function of the booster RF phase relative to the MMMG phase.

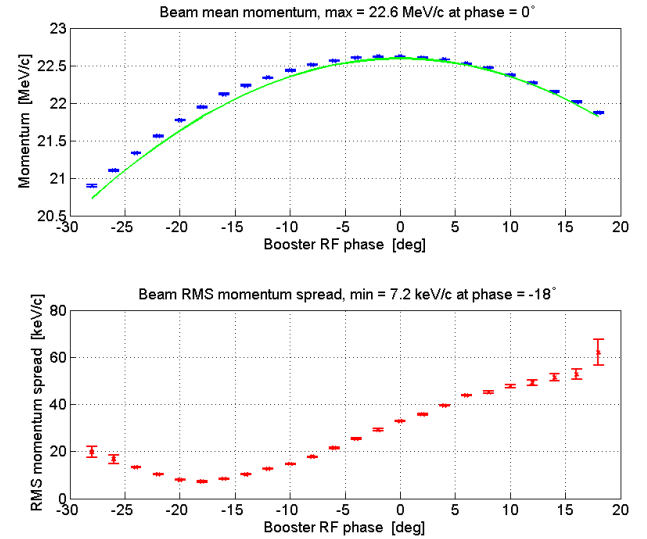


Figure 2: Top: the beam mean momentum as a function of the booster RF phase for 20 pC bunch charge and Gaussian laser temporal profile, blue dots with error bars show measurements; green curve shows acceleration model according Eq. (1). Bottom: RMS momentum spread shown as red dots with error bars, as a function of the booster RF phase.

The used booster RF phase range was from -28° to $+18^\circ$ with respect to the MMMG phase with a step width of 2 degrees. The maximum mean momentum gain from the

booster cavity was $V = (22.6 - 6.8) \text{ MeV/c} = 15.8 \text{ MeV/c}$, where 22.6 MeV/c is the maximum mean momentum downstream the booster and 6.8 MeV/c is the maximum mean momentum downstream the gun. As a result, the maximum momentum chirp k_{max} at the RF phase of $+18^\circ$ calculated according to Eq. (2), is 40 keV/c/ps , for $f = 1.3 \text{ GHz}$. The resulting temporal resolution σ_t of the reconstructed longitudinal phase space is about 0.25 ps or $75 \mu\text{m}$ for a slice momentum spread of the bunch $\sigma_\delta = 10 \text{ keV/c}$, Eq. (3). The result of the longitudinal phase space reconstruction using the ART algorithm is shown in Fig. 3.

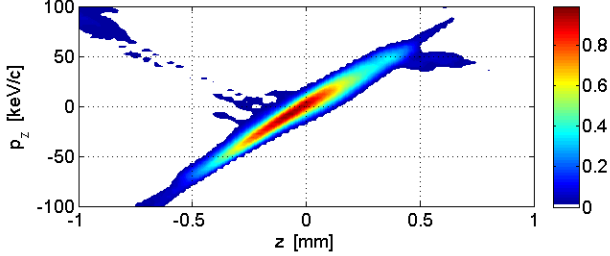


Figure 3: Reconstructed longitudinal phase space for a Gaussian temporal laser profile and 20 pC bunch charge.

Figure 4 shows the comparison of the bunch current profile, calculated from the reconstructed longitudinal phase space in Fig. 3, with the measured laser temporal profile. The current profile from Fig. 3 was calculated applying 15% charge cut to the reconstructed phase space in order to remove reconstruction artifacts.

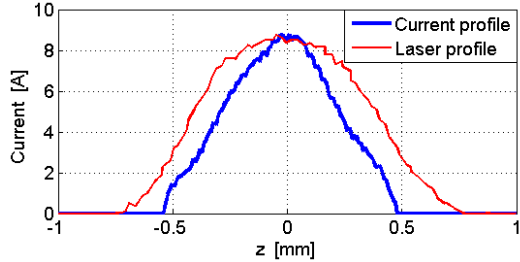


Figure 4: Current profile from Fig. 3, the blue curve, and the temporal laser profile, the red curve. The laser profile was scaled vertically to have the same amplitude as the current profile.

The calculated current profile is shorter than the laser profile (0.56 mm vs 0.86 mm at FWHM), due to three effects. Firstly, the charge cut applied to the phase space. Secondly, the weak tails of the distributions are not detected during the momentum measurements due to not perfect sensitivity of the measurement method. Thirdly, velocity bunching is taken place for low bunch charges at the initial acceleration in the gun when the electrons are started from the cathode surface. For the MMMG phase of the gun, the tail of the bunch sees a higher accelerating field than the head, resulting in bunch compression. For high charges the longitudinal space charge forces elongate the bunch.

The RMS bunch length calculated from the reconstruction is 0.22 mm . The rough estimation from the

momentum phase scan (Fig. 2) using Eq. (4) for the bunch momentum spread at $+18^\circ$ of $\delta_p = 60 \text{ keV/c}$ and for $V = 15.8 \text{ MeV/c}$, $k_0 = 40 \text{ keV/c/ps}$ calculated at $+18^\circ$ and $k_1 = 40 \text{ keV/c/ps}$ calculated at -18° gives the estimated bunch length of 0.23 mm . This number is reasonably close to the obtained value from the reconstructed current profile.

A second set of measurements was done for a bunch charge of 20 pC and a flat-top laser temporal profile with a FWHM length of 17.4 ps . Figure 5 shows the measured beam mean momentum and RMS momentum spread in the HEDA1 section as a function of the booster RF phase, relative to the MMMG phase. The used booster RF phase range was from -23° to $+22^\circ$ with respect to the MMMG phase with a step width of 1° . The beam maximum mean momentum gain from the booster cavity was $V = (22.3 - 6.8) \text{ MeV/c} = 15.5 \text{ MeV/c}$.

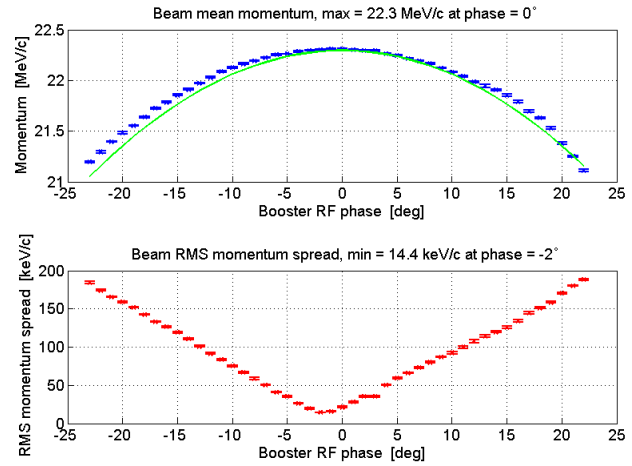


Figure 5: Top: the beam mean momentum as a function of the booster RF phase for 20 pC bunch charge and flat-top laser temporal profile, blue dots with error bars show measurements; green curve shows acceleration model according to Eq. (1). Bottom: RMS momentum spread shown as red dots with error bars, as a function of the booster RF phase.

The maximum momentum chirp applied to the bunch in this case is 47 keV/c/ps at the RF phase of $+22^\circ$, yielding a temporal resolution of 0.21 ps or $63 \mu\text{m}$. The reconstructed longitudinal phase space is shown in Fig. 6 and the comparison of the current profile with the laser profile is shown in Fig. 7.

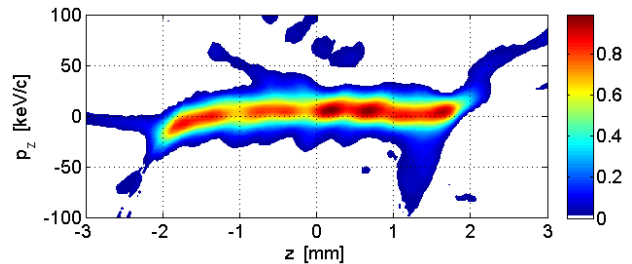


Figure 6: Reconstructed longitudinal phase space for flat-top temporal laser profile and 20 pC bunch charge.

The laser profile in Fig. 7 was squeezed longitudinally to have the same length and scaled vertically to have the same amplitude as the current profile for better comparison (original laser profile is longer). The modulation structure of the laser profile is well reproduced in the current profile and in the reconstructed phase space.

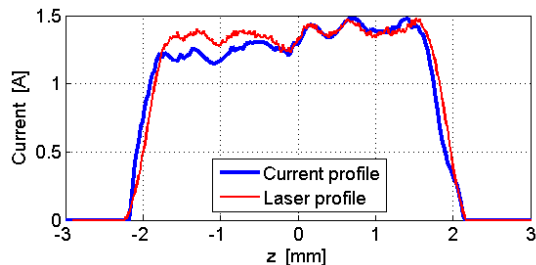


Figure 7: Current profile (the blue curve) and squeezed temporal laser profile (the red curve).

The RMS bunch length calculated from the reconstruction is 1.1 mm. The rough estimation from the momentum phase scan (Fig. 5) using Eq. (4) gives the same number.

CONCLUSION

The longitudinal phase space of the electron bunch can be measured using a tomographic technique by varying the RF phase of the acceleration structure. Such measurements were performed at the PITZ facility for two temporal laser profiles and 20 pC bunch charge. Reconstructed current profiles at low bunch charge are in good agreement with the measured temporal laser profiles, except that they are shorter due to velocity bunching. Temporal density modulations of the laser profile can be seen in the reconstructed longitudinal phase spaces. The bunch length can be quickly estimated from the momentum phase scan without performing the time consuming tomographic reconstruction.

REFERENCES

- [1] P. Schmueser, M. Dohlus and J. Rossbach, *Ultraviolet and Soft X-Ray Free-Electron Lasers*. (Springer, 2008).
- [2] P. Emma, *et al.*, A transverse RF Deflecting Structure for Bunch Length and Phase Space Diagnostics. LCLS-TN-00-12. 2000.
- [3] H. Loos, *et al.*, “Longitudinal phase space tomography at the SLAC Gun Test Facility and the BNL DUV-FEL”, Nucl. Instrum. Meth. A 528, (2004) 189.
- [4] D. Malyutin, *et al.*, “First results of a longitudinal phase space tomography at PITZ”, FEL2013, TUPSO47.
- [5] F. Stephan, C. H. Boulware, M. Krasilnikov, J. Bähr, *et al.*, “Detailed characterization of electron sources yielding first demonstration of European X-ray Free-Electron Laser beam quality.” Phys. Rev. ST Accel. Beams 13, 020704, (2010).
- [6] A.C. Kak, M. Slaney, *Principles of Computerized Tomographic Imaging*, (IEEE Press, 1979).
- [7] J. Le Duff, “Dynamics and acceleration in linear structures”, CERN Accelerator School, Fifth General Accelerator Physics Course, Jyväskylä, Finland, 7–18 September 1992, CERN 94-01.